Leptonic dark matter annihilation in the evolving universe: constraints and implications

Qiang Yuan[a,f], Bin Yue[b,f], Xiao-Jun Bi[c,a], Xuelei Chen[b,c], and Xinmin Zhang[d,e]

[a]*Key Laboratory of Particle Astrophysics, Institute of High Energy Physics,*

Chinese Academy of Science, Beijing 100049, P.R.China

[b]*National Astronomical Observatories,*

Chinese Academy of Sciences, Beijing 100012, P.R.China

[c]*Center for High Energy Physics, Peking University, Beijing 100871, P.R.China*

[d]*Theoretical Physics Division, Institute of High Energy Physics,*

Chinese Academy of Science, Beijing 100049, P.R.China

[e]*Theoretical Physics Center for Science Facilities (TPCSF),*

Chinese Academy of Science, Beijing 100049, P.R.China and

[f]*Graduate University of Chinese Academy of Sciences, Beijing 100049, P.R.China*

The cosmic electron and positron excesses have been explained as possible dark matter (DM) annihilation products. In this work we investigate the possible effects of such a DM annihilation scenario during the evolution history of the Universe. We first calculate the extragalactic γ-ray background (EGRB), which is produced through the final state radiation of DM annihilation to charged leptons and the inverse Compton scattering between electrons/positrons and the cosmic microwave background. The DM halo profile and the minimal halo mass, which are not yet well determined from the current N-body simulations, are constrained by the EGRB data from EGRET and Fermi telescopes. Then we discuss the impact of such leptonic DM models on cosmic evolution, such as the reionization and heating of intergalactic medium, neutral Hydrogen 21 cm signal and suppression of structure formation. We show that the impact on the Hydrogen 21 cm signal might show interesting signatures of DM annihilation, but the influence on star formation is not remarkable. Future observations of the 21 cm signals could be used to place new constraints on the properties of DM.

PACS numbers: 95.35.+d,95.85.Pw,98.58.Ge

I. INTRODUCTION

Recently, observations of the cosmic ray (CR) positron fraction by the PAMELA experiment [1], the total electron and positron spectra by the ATIC [2] experiment, the PPB-BETS [3] experiment, the HESS [4, 5] experiment and the Fermi [6] experiment all show interesting excesses when compared with the expectations of the conventional astrophysical background. Especially the PAMELA data confirm the hint of excess of positron fraction previously discovered by HEAT [7, 8] and AMS [9]. Many theoretical models have been proposed to explain these phenomena in past years, among which a class of leptonic dark matter (DM) annihilation models is of particular interest (e.g., [10, 11] or see the review [12]).

It was soon recognized that if DM annihilation can occur near the solar location to contribute to the locally observed CR leptons, it should occur everywhere in the Universe as long as DM exists. Shortly after the proposal of using DM annihilation to account for the data, the γ-ray and radio emissions from the Galactic center [13–15], the Milky Way halo [16–20], the dwarf galaxies [21–23], the galaxy clusters [24, 25] and the early Universe [26–28] were studied as possible constraints and/or future probes of the DM models. These studies have shown that the proposed DM scenarios are either excluded or at least strongly constrained if the DM halo properties derived from current numerical simulations are adopted. However, we should bear in mind that there are still large uncertainties in our understanding of the DM halo structure, especially for the small scales which are not yet probed by the current simulations due to the limited resolution. In the present work, we adopt the leptonic DM scenario implied from the CR data, and investigate what kind of constraint could be placed on the properties of dark matter halos [25, 29]. This exercise is useful in two ways. On one hand with the improvement of computing power and astrophysical observational precision, we will achieve better understanding of the DM halo, if in the future our DM-derived constraints are in conflict with these simulations or observations, then it helps to falsify the DM model considered here. On the other hand, it also helps to illustrate the possible model uncertainties in explaining the CR observations.

In this work we shall focus on the DM annihilation during the evolution history of the Universe, mainly after the epoch of cosmic recombination. The DM annihilation can produce electrons/positrons, which can scatter with the cosmic microwave background (CMB) photons to produce γ-rays and contribute to the extragalactic γ-ray background (EGRB). The

final state radiation (FSR) from DM annihilation into charged leptons (generated directly from the external legs of the Feynman diagram) can also contribute to the EGRB. Using the observations on the EGRB by EGRET [30] and most recently by Fermi [31], one can test the model configurations and constrain the model parameters [27, 28]. In addition, the energy of the final state particles from DM annihilation will be partially deposited in the baryonic gas, causing ionization and heating. This effect can be imprinted on the CMB anisotropy [32–37], the optical depth of CMB photons [38, 39], and the 21 cm signal from the neutral hydrogen during the dark age [40–42]. Furthermore, the heating also increases the Jeans mass, suppressing the accretion of gas into minihalos, and enhancing the photoevaporation of gas in minihalos [43]. These effects might affect the early star formation history of the Universe.

Different from previous studies, in this work we will normalize the particle physics parameters of DM particles (including mass, cross section, branching ratios etc.) to the recent observed CR lepton data [44][1], then calculate the EGRB and derive the constraints on the DM halo profile and the minimal halo mass using EGRET and Fermi data. Then we discuss the possible effects of DM annihilation on the ionization and heating of the intergalactic gas, the 21 cm signal and the early structure formation. Throughout this paper we will adopt the cosmological parameters from WMAP 5-yr results combined with the baryon acoustic oscillation and Type Ia supernova data: $\Omega_\chi = 0.228$, $\Omega_\Lambda = 0.726$, $\Omega_b = 0.046$, $h = 0.705$,$\sigma_8 = 0.812$ and $n_s = 0.96$ [45]. The uncertainties of the cosmological parameters would affect the detailed result of the clumpiness factor of DM. However, compared with the large uncertainties of other aspects in the study, e.g., the concentration model and structure formation history of DM, the uncertainties of cosmological parameters would play a negligible role.

II. EXTRAGALACTIC γ-RAY BACKGROUND

The γ-ray emission produced in the leptonic DM annihilation generally include two components: the inverse Compton (IC) component through interactions between electrons/positrons and the cosmological radiation field such as the CMB, and the direct FSR

---

[1] We adopt the parameters fitted using fixed background approach given in Ref. [44] (Table I).

associated with the annihilation process itself. The γ-ray flux observed at redshift z is obtained by integrating the emissivity through evolution history of the universe [38, 46],

$$\phi(E, z) = \frac{c(1+z)^2}{4\pi} \frac{\Omega_\chi^2 \rho_c^2 \langle \sigma v \rangle}{2m_\chi^2} \int_z^\infty \mathrm{d}z' \frac{(1+z')^3[\Delta^2(z')+1]}{H(z')} \frac{\mathrm{d}N}{\mathrm{d}E'} \exp\left[-\tau(z; z', E')\right], \quad (1)$$

where m_χ is the mass of DM particle, $\langle \sigma v \rangle$ is the velocity weighted annihilation cross section, $\rho_c = 3H_0^2/8\pi G$ is the critical density of the Universe at present, $H(z) = H_0\sqrt{(\Omega_\chi + \Omega_b)(1+z)^3 + \Omega_\Lambda}$ is the Hubble parameter. Here $E' \equiv E(1+z')/(1+z)$, and $\frac{\mathrm{d}N}{\mathrm{d}E'} = \frac{\mathrm{d}N}{\mathrm{d}E'}\big|_{\mathrm{IC}} + \frac{\mathrm{d}N}{\mathrm{d}E'}\big|_{\mathrm{FSR}}$ is the γ-ray generation multiplicity at redshift z' for one pair of annihilating DM particles. Note that the cascade contribution from pair production of the high energy photons interacting with CMB photons is not included. This treatment is reasonable due to the following two arguments. On one hand for the DM models considered in this work (see below Table I), the energy fraction that goes into FSR photons, which should be easier to reach the pair production threshold, is much smaller than that which goes into electrons/positrons. On the other hand, because of the large clumpiness factor the dominant contribution to the EGRB for most of the redshift range interested here (e.g., $z \lesssim 100$) comes from the DM annihilation at relatively low redshifts, where the pair production is also not important. The optical depth $\tau(z; z', E')$ of γ-ray photon with energy E', propagating from z' to z can be obtained as

$$\tau(z; z', E') = c \int_z^{z'} \mathrm{d}z'' \frac{\alpha(E'', z'')}{H(z'')(1+z'')}, \quad (2)$$

where $E'' = E'(1+z'')/(1+z')$, $\alpha(E, z)$ is the absorption coefficient. In this work we include the following interactions for photon propagation: the photo-ionization, photon-nuclei pair production, Compton scattering, photon-photon scattering and photon-photon pair production. The absorption coefficients of these processes are adopted from [47]. Note that for $6 \lesssim z \lesssim 1200$ the Universe is neutral, therefore the Compton scattering is negligible; otherwise when the Universe is ionized the photo-ionization is dropped. For redshift less than 6 we further include the pair production process between γ-ray photons and cosmic infrared background, using the optical depth of the "baseline" model in [48]. Finally $\Delta^2(z)$ is a factor describing the clumpiness of the DM structures. The detailed calculation of $\Delta^2(z)$ using structure formation theory is presented in the Appendix.

The FSR photon spectrum for the e^+e^- or $\mu^+\mu^-$ channel, when $m_\chi \gg m_e, m_\mu$, is given

by [49]

$$\left.\frac{\mathrm{d}N}{\mathrm{d}x}\right|^{i}_{\mathrm{FSR}} = \frac{\alpha}{\pi}\frac{1 + (1-x)^2}{x}\log\left(\frac{s}{m_i^2}(1-x)\right),$$ (3)

where $i = e, \mu$, $\alpha \approx 1/137$ is the fine structure constant, $s = 4m_\chi^2$ and $x = E/m_\chi$. For the $\tau^+\tau^-$ channel, there is an internal bremsstrahlung radiation from the chain $\tau \to \pi^0 \to \gamma$ in addition to the decay products. The total radiation is given by [50]

$$\left.\frac{\mathrm{d}N}{\mathrm{d}x}\right|^{\tau}_{\mathrm{FSR}} = x^{-1.31}\left(6.94x - 4.93x^2 - 0.51x^3\right)e^{-4.53x}.$$ (4)

The IC component of γ-ray photons is given by

$$\left.\frac{\mathrm{d}N}{\mathrm{d}E}\right|_{\mathrm{IC}} = \int \mathrm{d}\epsilon\, n(\epsilon) \int \mathrm{d}E_e \frac{\mathrm{d}n}{\mathrm{d}E_e} \times F_{\mathrm{KN}}(\epsilon, E_e, E),$$ (5)

where $n(\epsilon)$ is the photon number density of the background radiation as a function of energy ϵ, and $\frac{\mathrm{d}n}{\mathrm{d}E_e}$ is the quasi-equilibrium electron/positron energy spectrum from the DM annihilations. Following [28] we assume that the electrons/positrons lose their energies instantaneously after the production from DM annihilation,

$$\frac{\mathrm{d}n}{\mathrm{d}E_e} = \frac{1}{b(E_e, z)}\int_{E_e}^{m_\chi}\mathrm{d}E'_e\frac{\mathrm{d}N_e}{\mathrm{d}E'_e},$$ (6)

with the energy loss rate $b(E_e, z) \approx 2.67 \times 10^{-17}(1+z)^4 (E_e/\mathrm{GeV})^2$ GeV s^{-1}. Finally the differential Klein-Nishina cross section $F_{\mathrm{KN}}(\epsilon, E_e, E)$ in Eq.(5) is given by

$$F_{\mathrm{KN}}(\epsilon, E_e, E) = \frac{3\sigma_T}{4\gamma^2\epsilon}\left[2q\ln q + (1 + 2q)(1 - q) + \frac{(\Gamma q)^2(1-q)}{2(1 + \Gamma q)}\right],$$ (7)

with σ_T the Thomson cross section, γ the Lorentz factor of electron, $\Gamma = 4\epsilon\gamma/m_e$, and $q = \frac{E/E_e}{\Gamma(1-E/E_e)}$. For $q < 1/4\gamma^2$ or $q > 1$ we set $F_{\mathrm{KN}}(\epsilon, E_e, E) = 0$.

The calculated EGRB intensity is plotted in Fig. 1. Here we adopt two sets of DM particle parameters, as compiled in Table I, which are derived by a Markov Chain Monte Carlo (MCMC) fitting of the PAMELA+ATIC (Model I) and PAMELA+Fermi+HESS (Model II) data respectively [44]. The cross sections derived in [44] are based on a local DM density $\rho_\odot \approx 0.25 - 0.27$ GeV cm^{-3}, which seems to be smaller than the value derived in recent studies [51, 52]. Also, [53] shows that the dynamic measurements might systematically under-estimate the local density. A larger local density will result in a smaller cross section (by a factor of ~ 2) if we normalize the electron and positron fluxes to the observational excesses. Since the present work is more or less an order of magnitude study, we do not

expect the change of factor 2 will affect the qualitative conclusions in this work. But keep in mind that the signals discussed in the following should be recognized as upper limits of such scenarios.

The *Left* and *right* panels are for two concentration models of DM halos: Bullock et al. (B01, [54]) and Maccio et al. (M08, [55]) respectively. The expected EGRB intensity is a function of the DM halo parameters γ and M_{min} (see the Appendix). In this plot we adopt $\gamma = 1$ (NFW profile, [56]), and varying M_{min} from 10^7 M$_\odot$ to 10^{-6} M$_\odot$, corresponding to the observational lower limit of dwarf galaxies and theoretical lower limit of the cold DM scenario. It is shown that for B01 concentration the parameter settings with $M_{min} = 10^{-6}$ M$_\odot$ are allowed by EGRET data but marginally excluded by Fermi data. For M08 concentration model, the extension of halos to very low mass range seems to over produce γ-rays and conflict with both sets of data.

TABLE I: Mass, annihilation cross section and branching ratios of DM particles used in this work.

	m_χ	$\langle \sigma v \rangle$	B_e	B_μ	B_τ
	(TeV)	$(10^{-23}$ cm^{3}s$^{-1})$			
Model I	0.71	0.97	0.8	0.1	0.1
Model II	2.21	9.10	0.0	0.7	0.3

We then scan the two dimensional parameter space $M_{min} - \gamma$, and calculate the expected EGRB for each setting of parameters. By requring the calculated spectra not to exceed 2σ errorbars of the observational data, we derive the constraints on these two parameters, as shown in Fig. 2. The parameter space to the top-left side of each curve is excluded. The *left* panel is for B01 concentration model and the *right* panel is for M08 concentration model. In each panel we plot two groups of lines, corresponding to the EGRET and Fermi constraints respectively. We can see that the constraints are sensitive to the concentration models. The M08 concentration model were obtained by a power-law fitting in the high mass range and then extrapolated to the low mass range, while for B01 model the concentration of the low mass haloes shows an asymptotic flattening. So for M08 model the low mass haloes contribute more significantly to the γ-ray intensity than that of B01 model, hence the constraint is more stringent for M08 model when M_{min} is small.

From the results of the fitting, we find that the configuration of standard cold DM haloes,
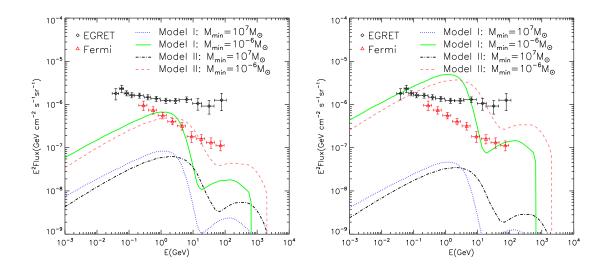
FIG. 1: EGRB from DM annihilation compared with the EGRET and Fermi data. *Left* panel is for B01 concentration, and the *right* panel is for M08 concentration model respectively. NFW halo profile is adopted.
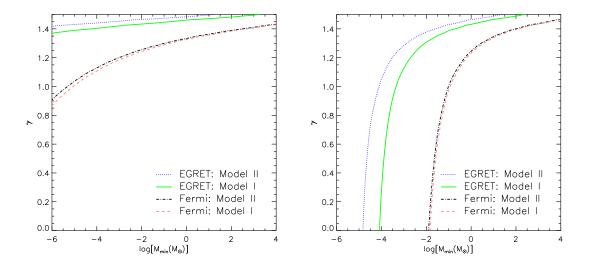

FIG. 2: Constraints on the DM halo parameters $M_{\min}$ and γ from EGRET and Fermi observations of EGRB. *Left* panel is for B01 concentration, and the *right* panel is for M08 concentration.

e.g., the NFW profile ($\gamma = 1$, [56]) and $M_{\min}$ down to $\sim 10^{-6}$ $M_{\odot}$, is constrained by the Fermi data. A warm DM scenario with non-thermal production of DM particles seems to

be safely consistent with the data[2][57].

III.   IMPLICATIONS

A.   Cosmic reionization and heating

Now we turn to the effects of DM annihilation on the cosmic reionization and heating. The energy deposited in the intergalactic medium (IGM) from DM annihilation can be expressed as [33]

$$\epsilon_{\rm DM}(z) = f(z) \left(\frac{\langle \sigma v \rangle \Omega_\chi^2 \rho_c^2}{2m_\chi^2 \, n_{\rm b0}} \right) (1+z)^3 \cdot 2m_\chi, \tag{8}$$

where $n_{\rm b0}$ is the present number density of baryon, and function $f(z)$ represents the efficiency of energy transfer from DM to the IGM. In [58] the efficiency $f(z)$ is calculated in detail and parameterized with fitting functions, without including the DM clumpiness. However, it can not be directly used with the existence of DM structures, because the mean free path of photons for some energies (e.g., $\sim$GeV) is large enough that the evolution of structures is necessary to be taken into account. In this work we follow the method given in [38] to calculate the energy deposition rate $f(z)$. In short $f(z)$ is defined as [38]

$$f(z) \equiv \frac{\int {\rm d}E\, E\phi(E, z)\alpha(E, z)}{\langle \sigma v \rangle \Omega_\chi^2 \rho_c^2 (1+z)^6 / m_\chi}, \tag{9}$$

where $\phi(E, z)$ is given by Eq. (1). The denominator of the above equation represents the energy output of DM annihilation without the clumpiness, and the numerator is the energy absorbed by IGM. Note here the energy transfer from DM annihilation to IGM is mainly due to the absorption of photons, no matter what the annihilation final state is. For details of the results of $f(z)$ please refer to [38]. Our calculated results are slightly different from that given in [38] due to different branching ratios of DM annihilation.

In addition to the energy injection from DM annihilation, X-rays can also heat the neutral IGM up to a high temperature [59–62]. We assume that the X-ray emissivity is proportional to the star formation rate, which at high redshifts is proportional to the differential increase of baryon collapse fraction [62] and is given by [63](see also [64]),

$$\epsilon_X(z) = 1.09 \times 10^{-31} f_X f_\star \left[\frac{\rho_{b,0}(1+z)^3}{{\rm M}_\odot {\rm Mpc}^{-3}} \right] \left| \frac{{\rm d}f_{\rm coll}}{{\rm d}z} \right| (1+z)hE(z) \; [{\rm eV\ cm}^{-3}{\rm s}^{-1}], \tag{10}$$

---

[2] See also the constraints derived in the Galactic center [29] and Virgo cluster [25].

where $E(z) = \sqrt{\Omega_m(1+z)^3 + \Omega_\Lambda}$, $f_X \sim 1.0$ is a renormalization factor, $f_\star$ is star formation efficiency and f_{coll} is the collapse fraction. We take $f_X = 1$ and $f_\star = 10^{-3}$.

Given the energy injection rate, the evolution equations of the ionization fractions and the IGM temperature are modified through adding the following terms to the standard equations [33]

$$-\delta\left(\frac{\mathrm{d}x_{\mathrm{H}}}{\mathrm{d}z}\right) = \frac{\epsilon_{\mathrm{DM}}(z) + \epsilon_{\mathrm{X}}(z)}{13.6\,\mathrm{eV}} \frac{1 - x_{\mathrm{H}}}{3(1 + f_{\mathrm{He}})} \frac{1}{H(z)(1+z)}, \tag{11}$$

$$-\delta\left(\frac{\mathrm{d}x_{\mathrm{He}}}{\mathrm{d}z}\right) = \frac{\epsilon_{\mathrm{DM}}(z) + \epsilon_{\mathrm{X}}(z)}{24.6\,\mathrm{eV}} \frac{1 - x_{\mathrm{He}}}{3(1 + f_{\mathrm{He}})} \frac{1}{H(z)(1+z)}, \tag{12}$$

$$-\delta\left(\frac{\mathrm{d}T_{\mathrm{igm}}}{\mathrm{d}z}\right) = \frac{2[\epsilon_{\mathrm{DM}}(z) + \epsilon_{\mathrm{X}}(z)]}{3} \frac{1 + 2x_{\mathrm{H}} + f_{\mathrm{He}}(1 + 2x_{\mathrm{He}})}{3(1 + f_{\mathrm{He}})} \frac{1}{H(z)(1+z)}, \tag{13}$$

where $f_{\mathrm{He}} \approx 0.083$ is the ratio of the number density of helium to that of hydrogen for the Universe, with the helium mass abundance $Y_{\mathrm{He}} = 0.25$. The ionization fraction of species A is defined as $x_A \equiv \frac{n_{A+}}{n_{A+}+n_A}$. These set of differential equations are solved using the RECFAST code [65].

In Fig. 3 we show the changes of the total ionization fraction $x_{\mathrm{ion}} = x_{\mathrm{H}} + f_{\mathrm{He}}x_{\mathrm{He}}$ and the IGM temperature as functions of redshift, in the presence of DM annihilation. The four curves correspond to the maximum clumpiness enhancement allowed by EGRET or Fermi data, for the two DM particle models. Actually, for different combinations of the parameters γ and M_{min} which lies on each of the curve in Fig. 2 the EGRB is of the same level. However, the impact on the ionization and heating histories could be slightly different. The parameters we chose in this study are compiled in Table II. Here we adopt the B01 concentration model and try to include as many low mass haloes as possible (i.e., the left end of each curve in Fig. 2).

TABLE II: The halo parameters used to calculate the reionization and heating processes. B01 concentration is adopted.

	Model I (EGRET)	Model II (EGRET)	Model I (Fermi)	Model II (Fermi)
γ	1.37	1.42	0.85	0.90
$M_{\mathrm{min}}(\mathrm{M}_\odot)$	10^{-6}	10^{-6}	10^{-6}	10^{-6}

We can see that at $z \approx 800$ the effects of DM annihilation on the recombination process begin to appear, which lead to a higher plateau of the cosmic ionization fraction. For $z \lesssim 50$
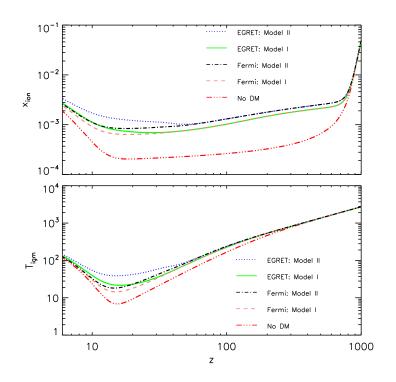
FIG. 3: The evolution of the cosmic ionization fraction (*upper* panel) and the IGM temperature (*lower* panel), under the constraints from EGRB.

the clumpiness enhancement becomes effective, which retards the decreasing trends of both the ionization fraction and IGM temperature. This shows that the DM annihilation may have obvious contributions to the ionization fraction of the Universe. However, it seems that the DM component is not able to fully ionize the Universe as suggested in [66], in order not to violate the EGRB observations. It is also shown in [38] that the model which can fully ionize the Universe will violate the CMB measurements.

This change of the recombination history will broaden the surface of last scattering, suppress the temperature fluctuations and enhance the polarization fluctuations of the CMB. A higher level of residual ionization fraction will also increase the scattering probability of CMB photons after decoupling, thus increasing the optical depth of CMB photons, which has been measured by WMAP [45]. The implications for the DM models from the above effects on the CMB were discussed recently in [38, 58]. Since these effects are not sensitive to the clumpiness factor $\Delta^2(z)$, we will not discuss them in detail here. We point out that the mass and cross section fitted in [44], and also used in the current study are consistent

with the WMAP constraints at 2σ level [58].

B. 21 cm signal from neutral Hydrogen

The redshifted 21 cm signal from neutral hydrogen can provide valuable information on the thermal state of gas in the dark ages. The differential brightness temperature relative to that of the CMB is given by

$$\delta T_b = 16(1 - x_{\rm H})(1 + \delta) \left(\frac{\Omega_b h}{0.02}\right) \left[\left(\frac{1+z}{10}\right)\left(\frac{0.3}{\Omega_m}\right)\right]^{1/2} \left[1 - \frac{T_{\rm CMB}(z)}{T_s}\right] [{\rm mK}], \qquad (14)$$

where $x_{\rm H}$ is the hydrogen ionization fraction as defined in the previous section, $T_{\rm CMB}(z)$ is the CMB temperature at redshift z, δ is the density contrast of the gas which should be 0 for the cosmic mean field[3], $\Omega_m = \Omega_\chi + \Omega_b$, and T_s is the spin temperature of the neutral hydrogen. The spin temperature, which describes the distribution on the two hyperfine-split ground states of neutral hydrogen, is given by a weighted average of the CMB temperature and gas kinetic temperature,

$$T_s = \frac{T_{\rm CMB}(z) + (y_{\alpha,{\rm eff}} + y_c)T_{\rm igm}}{1 + y_{\alpha,{\rm eff}} + y_c}. \qquad (15)$$

The weighting factor depends on the coupling between the spin system with atoms, which are induced either by atom-atom, atom-proton and atom-electron collisions (y_c), or by resonance scattering of the Lyα photons ($y_{\alpha,{\rm eff}}$) which has a color temperature almost equal to the gas kinetic temperature. Here we adopt y_c from [68] (see also the original references therein). The effective Lyα efficiency is

$$y_{\alpha,{\rm eff}} = \frac{P_{10}T_\star}{A_{10}T_{\rm igm}} \times e^{-0.3(1+z)^{1/2}T_{\rm igm}^{-2/3}} \left(1 + \frac{0.4}{T_{\rm igm}}\right)^{-1}, \qquad (16)$$

in which $T_\star = 0.068$ K corresponds to the energy split of the hyperfine structures of neutral hydrogen, $P_{10} \approx 1.3 \times 10^9 J_\alpha$ with J_α the specific intensity of Lyα radiation, and $A_{10} = 2.85 \times 10^{-15}$ s^{-1} is the Einstein coefficient of the hyperfine spontaneous transition (see [69, 70]).

---

[3] This formula neglects the effect from peculiar velocity, the spherical average of peculiar velocity correction would give a factor $4/3$ in front of δ [67], however, it does not affect our calculation since we consider the 21 cm signal of the cosmic mean field, i.e. $\delta = 0$.
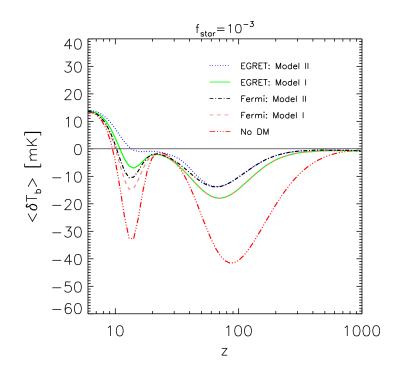
FIG. 4: Evolution of the 21 cm signal for the four different DM models, compared with the case without DM annihilation. In all cases, heating from X-ray and Lyα photons from stars are included, see the text for details. The thin solid line corresponds to $\delta T_b = 0$.

We firstly consider the standard picture without the energy injection from DM annihilation. During the dark age, the scattering of residual free electrons with CMB photons will keep the gas temperature comparable with the CMB temperature at the initial stage. After kinetic decoupling of the baryons from radiation at $z \sim 200$, the gas temperature drops faster, i.e. $T_{igm} \sim (1+z)^{-2}$. The mean density of the Universe is still high at this time, and the coupling due to collisions is strong enough to make T_s almost equal to T_{igm}, so we would see an absorption 21 cm signal (c.f. the line labeled "No DM" in Fig. 4). This absorptional signal peaks at $z \sim 100$. As the redshift decreases, the density drops and the collisional coupling becomes less effective, resulting in the spin temperature approaches $T_{CMB}(z)$ and the 21 cm absorption signal becomes weak. However, as the stars begin to form, Lyα photons are produced, and the spin temperature deviates from $T_{CMB}(z)$ and gets close to T_{igm} again. Thus before the IGM is heated above the CMB temperature, we would see a second absorption peak. The location of the second peak depends on the model of

star formation, Lyα and X-ray production rate [59]. We model the production of the Lyα background by star formation following Ref. [71]. The evolution of the Lyα background is plotted in Fig. 5. The contribution to Lyα from star formation rises sharply after $z \sim 40$. This model is very simple but illustrates qualitatively the main feature of the 21 cm signal evolution. For our adopted model, the second absorption peak is at $z \sim 14$. The signal converts from absorption to emission at $z \sim 10$ due to X-ray heating.

In the above we described the case of the global signal according to the mean density of gas. In addition, minihalos are formed during the late dark ages. Within minihalos the temperature of the gas is higher and the spin-kinetic coupling is also maintained by collisions as the density is higher. The minihalos could produce a positive 21 cm signal, but even taking into account the contribution from minihalos, the overall absorption signal is still apparent [61, 72, 73].
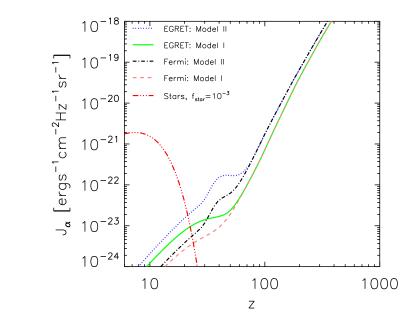

FIG. 5: Evolution of the DM induced Lyα intensity. For comparison, we also plot the Lyα intensity from stars in the same panel. DM annihilation provides an early Lyα background, but the contribution from stars increases dramatically after redshift $z \approx 30$.

Now we turn to the cases with DM annihilation. The annihilation of DM has two effects

on the 21 cm signal. On one hand, it heats the IGM up to a higher temperature and causes a partial ionization, as shown in Fig. 3. On the other hand, it also produces an early Lyα background before the formation of the first stars through de-excitation. The evolutions of δT_b for different DM models as listed in Table II are plotted in Fig. 4. The transition redshift at which the IGM temperature exceeds the CMB temperature is also the redshift at which the 21 cm signal changes from absorption to emission.

Assuming that a fraction f_α of the excitation energy goes into Lyα photons, the evolution of Lyα intensity is

$$J_\alpha = \frac{c}{4\pi} \frac{[1 - x_H + f_{He}(1 - x_{He})]}{3(1 + f_{He})} f_\alpha \, \epsilon_{DM}(z) \frac{n_b}{\nu_\alpha H(z)}, \tag{17}$$

where n_b is the number density of baryon, $\nu_\alpha = 2.47 \times 10^{15}$ Hz is the frequency of Lyα photon. We adopt the energy conversion fraction $f_\alpha = 0.5$ [40, 42]. The evolution of the DM annihilation induced Lyα intensity is shown in Fig. 5 for different models. The DM annihilation produces a Lyα flux even during the dark ages. As the Universe expands and the DM density falls, the Lyα flux decreases due to the drop of annihilation rate. Thanks to the structure formation J_α shows some enhancement for $z < 80$. Due to the expansion of the Universe, however, the flux which is proportional to the proper density of the photons still shows a trend of decrease, and the emission from the stars dominates at lower redshift.

The 21 cm signal with leptonic DM annihilation contribution is shown in Fig. 4. During the dark age, the absorption signal would not be as strong as the case without DM annihilation, because the IGM is heated to higher temperatures. Also the second absorption peak will become weaker due to the enhancement of DM structures. In some case there is even no 2nd absorption peak. The transition redshift from absorption to emission will be different from the case without DM annihilation. However, because there is large uncertainty of the impact on 21 cm signal from stars, it is not easy to use the transition redshift to distinguish the model with DM annihilation from the standard one. We conclude that the magnitude of the first absorption peak will be more efficient to search for the DM annihilation signal and constrain the DM models.

C.   Suppression on structure formation

Heating by DM annihilation can also suppress the accretion of gas by haloes. The minimum mass for a halo to accrete gas from environment is the Jeans mass,

$$M_J = \frac{\pi}{6} \left(\frac{\pi k_B T_{\text{igm}}}{G \mu m_H} \right)^{3/2} \rho^{-1/2}, \tag{18}$$

where μ is the averaged particle weight, G is the gravitational constant, k_B is Boltzmann constant and m_H is the mass of hydrogen atom (see [43]). The Jeans mass depends on the temperature of the gas. In the adiabatic model the temperature of the gas would decrease as redshift decreases. As a result the Jeans mass would be lower. However, with the heating of IGM by DM annihilations, the Jeans mass would instead increase at lower redshift, as shown in the left panel of Fig. 6.

Without external heating, it is thought that the first stars (population III or Pop III) might be formed in DM halos with a virial temperature above 10^3 K (corresponding to halos with mass $\sim 10^5$ M$_\odot$ at $z \sim 30$). In such halos the trace amount of H$_2$ in the primordial gas could cool the accreted gas, which would be bound further and form stars. With the existence of DM annihilation, the IGM gas will be heated up to higher temperatures, and the corresponding Jeans mass will also become higher. However, as shown in Fig. 6 the Jeans mass will be lower than mass with virial temperature 10^3 K, which means the impact on the formation of the first stars may be weak.

To account for the effect of DM annihilation on early star formation, we also follow the prescription given by Oh & Haiman [74] to estimate the fraction of gas (f_{gas}) left in a halo in the presence of an "entropy floor", i.e. heating of the gas by an external source. This fraction is determined by $\hat{K} = K_{\text{IGM}}/K_o$, where $K_{\text{IGM}} = T_{\text{IGM}}(z)/n^{2/3}(z)$ is the entropy of the IGM, and $K_o = T_{\text{vir}}/n^{2/3}(r_{\text{vir}})$ is the entropy of a halo at the virial radius. We interpolate f_{gas} as a function of $\hat{K}$ following [74] (see also [61]), adopting $\gamma = 1$ (i.e. NFW profile). The *right* panel of Fig. 6 shows the evolution of the minimum mass of halos that can retain at least 20% of the gas. This mass is several times larger than the Jeans mass, however, it is still less than the virial mass supposed to form the first stars. The DM annihilation is shown not to significantly affect the early star formation.
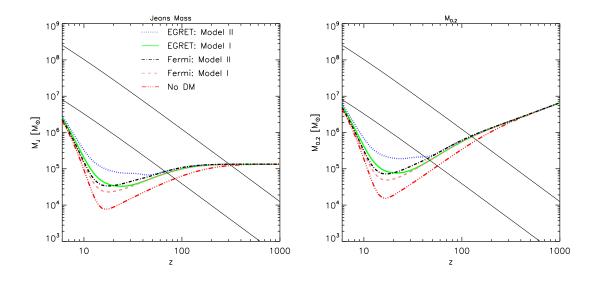
FIG. 6: Jeans mass (*left*) and the minimum mass of a halo that can hold at least 20% of gas (*right*) for different DM models. The two thin solid lines correspond to the virial mass of halo with $T_{\rm vir} = 10^3$ K (*lower*) and $T_{\rm vir} = 10^4$ K (*upper*) respectively.

IV.   CONCLUSIONS AND DISCUSSIONS

In this work we investigate the leptonic DM annihilation, as indicated by the recent CR lepton data from PAMELA, ATIC, HESS and Fermi, during the evolution process of the Universe. We mainly focus on the period after the cosmic recombination. The mass of DM particle, annihilation cross section and branching ratios to three lepton flavors are adopted to best-fit the observational CR lepton data in the Galaxy. Then we calculate the expected EGRB flux from DM annihilation, including FSR and electron/positron IC emission. The DM clumpiness effect is included in the calculation according to the Sheth-Tormen (ST) halo mass function [75]. Two free parameters, the central density slope γ and the minimum halo mass $M_{\rm min}$, are employed to describe the properties of the DM halo. Even so, the DM halo still suffers the uncertainties of the concentration. We adopt two kinds of concentration models in this work, B01 [54] and M08 [55].

The calculated EGRB results are compared with the observational data from EGRET and Fermi. By requiring the calculated EGRB not to exceed 2σ errorbars of the data, we can get a conservative constraint on parameters γ and $M_{\rm min}$. We find that for the B01

concentration model, the constraints on the model parameters are relatively weak, while for M08 concentration model in which the concentration of low mass halo is very large, the constraints are much stronger. Fermi data can give much stronger constraints than EGRET data. Even for B01 concentration, Fermi data can constrain the canonical cold DM prediction of halos, e.g. $\gamma = 1$ and $M_{\min} \approx 10^{-6}$ $M_{\odot}$. Since the spectral shape of the DM contribution is obviously different from the observational one, we would expect that the DM component does not contribute significantly to the EGRB. Therefore taking into account the background contribution we can expect that the remaining possible DM can be much reduced. We suggest that a warm DM scenario with non-thermal production of DM particles [57] might be consistent with the data safely.

Then we investigate the effects of such models of DM annihilation on the reionization and heating of the IGM. In our model, in the absence of DM annihilation but with X-ray only, the ionization fraction and the IGM temperature till $z \approx 6$ are $O(10^{-3})$ and $O(100)$ K respectively[4]. If the DM annihilation is taken into account as an energy source, the cosmic ionization fraction will have a higher plateau (of the order $O(10^{-3})$) during the evolution history. Also the IGM temperature will be higher by several times for redshift $10 < z < 100$. However, the effects of DM clumpiness on the enhancement of the energy deposition rate are not effective. In our treatment the energy deposition process within the evolution frame of the Universe is taken into account, which will result in a much lower energy deposition rate compared with the case with instantaneous energy deposition. We further find that it is impossible for the DM models considered here to fully ionize the Universe without conflicting with the EGRB data.

Finally we discuss the influence of the DM annihilation on the neutral hydrogen 21 cm signal and the suppression on structure formation, which may connect with observations more directly than the ionization fraction and the IGM temperature. It is found that the global 21 cm signal for the models with DM annihilation differs somewhat from the "standard" scenario without DM annihilation. Due to the rise of the IGM temperature

---

[4] Note that the ionization fraction seems to be lower than that derived according to observations of Lyα forest and the WMAP measurement of the electron scattering optical depth [76]. In this work we only adopt a simple description of the ordinary reionization precess and do not intend to give good description to Lyα forest and WMAP data. In fact, there are still large uncertainties on the meansurements of mean transmittance of Lyα flux, especially at high redshifts. A detailed model of the reionization history based on the Lyα and WMAP observations is strongly model dependent and out of the purpose of this study.

during the dark age, the 21 cm absorption signal is much smaller than the "standard" case. Also, the Lyα flux supplied by the DM annihilation would make the spin temperature be closer to the gas kinetic temperature at $z < 40$. But again due to the heating, the gas kinetic temperature could exceed CMB temperature earlier than the "standard" case. In some model the $2nd$ absorption peak with redshift between 10 and 20 in the "standard" scenario may not appear. Future 21 cm observations may have the potential to test this leptonic DM annihilation scenario and constrain the model parameters, despite the technical difficulty in practice.

The heating of the IGM will also affect the Jeans mass, which characterizes the critical mass of DM halo that can accrete gas. We show that with the constraint from EGRB observations, the leptonic DM annihilation scenarios are not able to affect the structure formation process significantly.

Appendix: Clumpiness enhancement factor of DM annihilation

The density profile of a DM halo with mass $M_{\rm vir}$ can be parameterized as

$$\rho(r) = \frac{\rho_s}{(r/r_s)^\gamma (1 + r/r_s)^{3-\gamma}} = \rho_s \times \tilde{\rho}(x \equiv r/r_s), \tag{A.1}$$

here we adopt a free parameter γ to represent the inner profile of DM distribution inside a halo. The scale radius r_s is determined by the concentration parameter $c_{\rm vir}$ of the halo

$$r_s = \frac{r_{\rm vir}}{c_{\rm vir}(2 - \gamma)}, \tag{A.2}$$

where

$$r_{\rm vir} = \left(\frac{3 M_{\rm vir}}{4\pi \Delta_{\rm vir}(z) \rho_\chi(z)} \right)^{1/3}, \tag{A.3}$$

is the virial radius, with $\rho_\chi(z) = \rho_\chi(1+z)^3$ the DM density at redshift z, $\Delta_{\rm vir}(z) = (18\pi^2 + 82y - 39y^2)/(1 + y)$, $y = \Omega_m(z) - 1$ and $\Omega_m(z) = \frac{\Omega_m(1+z)^3}{\Omega_m(1+z)^3 + \Omega_\Lambda}$ [77]. The concentration parameter as a function of halo mass $M_{\rm vir}$ can be extracted from N-body simulations. For the low mass halos which are beyond the resolution of simulations, the concentration is obtained by extrapolation.In this paper we considered two extrapolation models. One is the analytical model developed in Ref. [54] (B01), and the other is the direct extrapolation of the fitting results from simulations under the WMAP5 cosmology [55] (M08). For both

models we employ the redshift evolution $c_{\mathrm{vir}}(z) = c_{\mathrm{vir}}(z=0)/(1+z)$ [54]. The scale density ρ_s is determined by normalizing the mass of the halo to M_{vir}.

The annihilation γ-ray intensity from a single halo is

$$
\begin{aligned}
L(M_{\mathrm{vir}}) &= 4\pi \int_0^{r_{\mathrm{vir}}} \rho^2(r) r^2 \mathrm{d}r \\
&= 4\pi r_s^3 \rho_s^2 \int_0^{x_{\max}} \tilde{\rho}^2(x) x^2 \mathrm{d}x \\
&= \frac{M_{\mathrm{vir}} \Delta_{\mathrm{vir}}(z) \rho_\chi(z) x_{\max}^3}{3} \frac{\int \tilde{\rho}^2(x) x^2 \mathrm{d}x}{\left(\int \tilde{\rho}(x) x^2 \mathrm{d}x\right)^2},
\end{aligned}
\tag{A.4}
$$

where $x_{\max} = c_{\mathrm{vir}}(2-\gamma)$. For a population of DM halos with comoving number density distribution $\mathrm{d}n(z)/\mathrm{d}M_{\mathrm{vir}}$ the total annihilation luminosity is

$$
L_{\mathrm{tot}} = \int \mathrm{d}M_{\mathrm{vir}} \frac{\mathrm{d}n(z)}{\mathrm{d}M_{\mathrm{vir}}}(1+z)^3 L(M_{\mathrm{vir}}) = \rho_\chi^2 (1+z)^6 \times \Delta^2(z),
\tag{A.5}
$$

in which one of the $(1+z)^3$ factor comes from $\rho_\chi(z)$ term in Eq.(A.4), and the other $(1+z)^3$ converts the comoving halo mass function to the physical one. In the above equation we define the clumpiness enhancement factor as

$$
\Delta^2(z) = \frac{\Delta_{\mathrm{vir}}(z)}{3\rho_\chi} \int \mathrm{d}M_{\mathrm{vir}} M_{\mathrm{vir}} \frac{\mathrm{d}n(z)}{\mathrm{d}M_{\mathrm{vir}}} \frac{\int \tilde{\rho}^2(x) x^2 \mathrm{d}x}{\left(\int \tilde{\rho}(x) x^2 \mathrm{d}x\right)^2} x_{\max}^3.
\tag{A.6}
$$

This is used in Eq. (1).

Finally we specify the halo mass function. The comoving number density distribution of DM haloes can be expressed as

$$
\frac{\mathrm{d}n(z)}{\mathrm{d}M_{\mathrm{vir}}} = \frac{\rho_\chi}{M_{\mathrm{vir}}} \sqrt{\frac{2A^2 a^2}{\pi}} \left[1 + (a\nu^2)^{-p}\right] \exp\left(-a\nu^2/2\right) \frac{\mathrm{d}\nu}{\mathrm{d}M_{\mathrm{vir}}},
\tag{A.7}
$$

where $\nu = \delta_c(z)/\sigma(M_{\mathrm{vir}})$, $\delta_c(z) = 1.68/D(z)$ is the critical overdensity in spherical collapse model, $D(z)$ is the linear growth factor [78]. A, a and p are constants. For $(A, a, p) = (0.5, 1, 0)$ it is the Press-Schechter (PS) formula [79], and for $(A, a, p) = (0.322, 0.707, 0.3)$ it is Sheth-Tormen (ST) formula [75]. In this work we adopt the ST mass function. $\sigma^2(M_{\mathrm{vir}})$ is the average variance of density field

$$
\sigma^2(M_{\mathrm{vir}}) = \frac{1}{2\pi^2} \int W^2(kR_{\mathrm{M}}) P_\delta(k) k^2 \mathrm{d}k,
\tag{A.8}
$$

with the top-hat window function $W(x) = 3(\sin x - x\cos x)/x^3$. $R_{\mathrm{M}} = (3M_{\mathrm{vir}}/4\pi\rho_m)^{1/3}$ is a radius within which a mass M_{vir} is contained with a uniform matter density field. The matter power spectrum $P_\delta(k)$ is expressed as

$$
P_\delta(k) = A_s (k \cdot \mathrm{Mpc})^{n_s} T^2(k),
\tag{A.9}
$$

where A_s is normalized using σ_8, transfer function $T(k)$ is obtained from a fit of CDM model [80],

$$T(q) = \frac{\ln(1 + 2.34q)}{2.34q} \left[1 + 3.89q + (16.1q)^2 + (5.46q)^3 + (6.71q)^4\right]^{-0.25} \tag{A.10}$$

with $q = k/h\Gamma$ and $\Gamma = \Omega_m h \exp[-\Omega_b(1 + \sqrt{2h}/\Omega_m)]$.

Acknowledgments

[1] O. Adriani, G. C. Barbarino, G. A. Bazilevskaya, R. Bellotti, M. Boezio, E. A. Bogomolov, L. Bonechi, M. Bongi, V. Bonvicini, S. Bottai, et al., Nature **458**, 607 (2009), 0810.4995.

[2] J. Chang, J. H. Adams, H. S. Ahn, G. L. Bashindzhagyan, M. Christl, O. Ganel, T. G. Guzik, J. Isbert, K. C. Kim, E. N. Kuznetsov, et al., Nature **456**, 362 (2008).

[3] S. Torii, T. Yamagami, T. Tamura, K. Yoshida, H. Kitamura, K. Anraku, J. Chang, M. Ejiri, I. Iijima, A. Kadokura, et al., ArXiv e-prints: 0809.0760 (2008), 0809.0760.

[4] F. Aharonian, A. G. Akhperjanian, U. Barres de Almeida, A. R. Bazer-Bachi, Y. Becherini, B. Behera, W. Benbow, K. Bernlöhr, C. Boisson, A. Bochow, et al., Phys. Rev. Lett. **101**, 261104 (2008), 0811.3894.

[5] F. Aharonian, A. G. Akhperjanian, G. Anton, U. Barres de Almeida, A. R. Bazer-Bachi, Y. Becherini, B. Behera, K. Bernlöhr, A. Bochow, C. Boisson, et al., Astron. Astrophys. **508**, 561 (2009).

[6] A. A. Abdo, M. Ackermann, M. Ajello, W. B. Atwood, M. Axelsson, L. Baldini, J. Ballet, G. Barbiellini, D. Bastieri, M. Battelino, et al., Phys. Rev. Lett. **102**, 181101 (2009), 0905.0025.

[7] S. W. Barwick, J. J. Beatty, A. Bhattacharyya, C. R. Bower, C. J. Chaput, S. Coutu, G. A. de Nolfo, J. Knapp, D. M. Lowder, S. McKee, et al., Astrophys. J. Lett. **482**, L191 (1997), arXiv:astro-ph/9703192.

[8] J. J. Beatty, A. Bhattacharyya, C. Bower, S. Coutu, M. A. Duvernois, S. McKee, S. A. Minnick, D. Müller, J. Musser, S. Nutter, et al., Phys. Rev. Lett. **93**, 241102 (2004), arXiv:astro-ph/0412230.

[9] M. Aguilar, J. Alcaraz, J. Allaby, B. Alpat, G. Ambrosi, H. Anderhub, L. Ao, A. Arefiev, P. Azzarello, L. Baldini, et al., Phys. Lett. B **646**, 145 (2007), arXiv:astro-ph/0703154.

[10] L. Bergström, T. Bringmann, and J. Edsjö, Phys. Rev. D **78**, 103520 (2008), 0808.3725.

[11] M. Cirelli, M. Kadastik, M. Raidal, and A. Strumia, Nuclear Physics B **813**, 1 (2009), 0809.2409.

[12] X. He, Modern Physics Letters A **24**, 2139 (2009), 0908.2908.

[13] G. Bertone, M. Cirelli, A. Strumia, and M. Taoso, Journal of Cosmology and Astro-Particle Physics **3**, 9 (2009), 0811.3744.

[14] J. Zhang, X. J. Bi, J. Liu, S. M. Liu, P. F. Yin, Q. Yuan, and S. H. Zhu, Phys. Rev. D **80**, 023007 (2009), 0812.0522.

[15] L. Bergström, G. Bertone, T. Bringmann, J. Edsjö, and M. Taoso, Phys. Rev. D **79**, 081303 (2009), 0812.3895.

[16] E. Borriello, A. Cuoco, and G. Miele, Astrophys. J. Lett. **699**, L59 (2009), 0903.1852.

[17] M. Cirelli and P. Panci, Nuclear Physics B **821**, 399 (2009), 0904.3830.

[18] M. Regis and P. Ullio, Phys. Rev. D **80**, 043525 (2009), 0904.4645.

[19] J. Zhang, Q. Yuan, and X. J. Bi, ArXiv e-prints (2009), 0908.1236.

[20] M. Cirelli, P. Panci, and P. D. Serpico, ArXiv e-prints (2009), 0912.0663.

[21] L. Pieri, M. Lattanzi, and J. Silk, Mon. Not. Roy. Astron. Soc. **399**, 2033 (2009), 0902.4330.

[22] R. Essig, N. Sehgal, and L. E. Strigari, Phys. Rev. D **80**, 023506 (2009), 0902.4750.

[23] M. Kuhlen, Advances in Astronomy **2010** (2010), 0906.1822.

[24] T. E. Jeltema, J. Kehayias, and S. Profumo, Phys. Rev. D **80**, 023005 (2009), 0812.0597.

[25] A. Pinzke, C. Pfrommer, and L. Bergström, Phys. Rev. Lett. **103**, 181302 (2009), 0905.1948.

[26] M. Kamionkowski and S. Profumo, Phys. Rev. Lett. **101**, 261301 (2008), 0810.3233.

[27] M. Kawasaki, K. Kohri, and K. Nakayama, Phys. Rev. D **80**, 023517 (2009), 0904.3626.

[28] S. Profumo and T. E. Jeltema, Journal of Cosmology and Astro-Particle Physics **7**, 20 (2009),

0906.0001.

[29] X. Bi, R. Brandenberger, P. Gondolo, T. J. Li, Q. Yuan, and X. M. Zhang, Phys. Rev. D **80**, 103502 (2009), 0905.1253.

[30] P. Sreekumar, D. L. Bertsch, B. L. Dingus, J. A. Esposito, C. E. Fichtel, R. C. Hartman, S. D. Hunter, G. Kanbach, D. A. Kniffen, Y. C. Lin, et al., Astrophys. J. **494**, 523 (1998), arXiv:astro-ph/9709257.

[31] A. A. Abdo, M. Ackermann, M. Ajello, W. B. Atwood, L. Baldini, J. Ballet, G. Barbiellini, D. Bastieri, B. M. Baughman, K. Bechtol, et al., Physical Review Letters **104**, 101101 (2010).

[32] X. Chen and M. Kamionkowski, Phys. Rev. D **70**, 043502 (2004), arXiv:astro-ph/0310473.

[33] N. Padmanabhan and D. P. Finkbeiner, Phys. Rev. D **72**, 023508 (2005), arXiv:astro-ph/0503486.

[34] L. Zhang, X. Chen, Y.-A. Lei, and Z.-G. Si, Phys. Rev. D **74**, 103519 (2006), arXiv:astro-ph/0603425.

[35] M. Mapelli, A. Ferrara, and E. Pierpaoli, Mon. Not. Roy. Astron. Soc. **369**, 1719 (2006), arXiv:astro-ph/0603237.

[36] S. Galli, F. Iocco, G. Bertone, and A. Melchiorri, Phys. Rev. D **80**, 023505 (2009), 0905.0003.

[37] T. Kanzaki, M. Kawasaki, and K. Nakayama, ArXiv e-prints (2009), 0907.3985.

[38] G. Hütsi, A. Hektor, and M. Raidal, Astron. Astrophys. **505**, 999 (2009), 0906.4550.

[39] M. Cirelli, F. Iocco, and P. Panci, Journal of Cosmology and Astro-Particle Physics **10**, 9 (2009), 0907.0719.

[40] S. R. Furlanetto, S. P. Oh, and E. Pierpaoli, Phys. Rev. D **74**, 103502 (2006), arXiv:astro-ph/0608385.

[41] L. Chuzhoy, Astrophys. J. Lett. **679**, L65 (2008), 0710.1856.

[42] A. Natarajan and D. J. Schwarz, Phys. Rev. D **80**, 043529 (2009), 0903.4485.

[43] E. Ripamonti, M. Mapelli, and A. Ferrara, Mon. Not. Roy. Astron. Soc. **375**, 1399 (2007), arXiv:astro-ph/0606483.

[44] J. Liu, Q. Yuan, X. Bi, H. Li, and X. Zhang, Phys. Rev. D **81**, 023516 (2010), 0906.3858.

[45] E. Komatsu, J. Dunkley, M. R. Nolta, C. L. Bennett, B. Gold, G. Hinshaw, N. Jarosik, D. Larson, M. Limon, L. Page, et al., Astrophys. J. Supp. **180**, 330 (2009), 0803.0547.

[46] P. Ullio, L. Bergström, J. Edsjö, and C. Lacey, Phys. Rev. D **66**, 123502 (2002), arXiv:astro-ph/0207125.

[47] A. A. Zdziarski and R. Svensson, Astrophys. J. **344**, 551 (1989).

[48] F. W. Stecker, M. A. Malkan, and S. T. Scully, Astrophys. J. **648**, 774 (2006), arXiv:astro-ph/0510449.

[49] L. Bergström, T. Bringmann, M. Eriksson, and M. Gustafsson, Phys. Rev. Lett. **94**, 131301 (2005), arXiv:astro-ph/0410359.

[50] N. Fornengo, L. Pieri, and S. Scopel, Phys. Rev. D **70**, 103529 (2004), arXiv:hep-ph/0407342.

[51] R. Catena and P. Ullio, J. Cosmo. Astropart. Phys. **8**, 4 (2010), 0907.0018.

[52] P. Salucci, F. Nesti, G. Gentile, and C. F. Martins, ArXiv e-prints (2010), 1003.3101.

[53] M. Pato, O. Agertz, G. Bertone, B. Moore, and R. Teyssier, Phys. Rev. D **82**, 023531 (2010), 1006.1322.

[54] J. S. Bullock, T. S. Kolatt, Y. Sigad, R. S. Somerville, A. V. Kravtsov, A. A. Klypin, J. R. Primack, and A. Dekel, Mon. Not. Roy. Astron. Soc. **321**, 559 (2001), arXiv:astro-ph/9908159.

[55] A. V. Macciò, A. A. Dutton, and F. C. van den Bosch, Mon. Not. Roy. Astron. Soc. **391**, 1940 (2008), 0805.1926.

[56] J. F. Navarro, C. S. Frenk, and S. D. M. White, Astrophys. J. **490**, 493 (1997), arXiv:astro-ph/9611107.

[57] W. B. Lin, D. H. Huang, X. Zhang, and R. Brandenberger, Phys. Rev. Lett. **86**, 954 (2001), arXiv:astro-ph/0009003.

[58] T. R. Slatyer, N. Padmanabhan, and D. P. Finkbeiner, Phys. Rev. D **80**, 043526 (2009), 0906.1197.

[59] X. Chen and J. Miralda-Escudé, Astrophys. J. **602**, 1 (2004), arXiv:astro-ph/0303395.

[60] S. R. Furlanetto, S. P. Oh, and F. H. Briggs, Phys. Rept. **433**, 181 (2006), arXiv:astro-ph/0608032.

[61] S. R. Furlanetto and S. P. Oh, Astrophys. J. **652**, 849 (2006), arXiv:astro-ph/0604080.

[62] X. Chen and J. Miralda-Escudé, Astrophys. J. **684**, 18 (2008), arXiv:astro-ph/0605439.

[63] S. R. Furlanetto, Mon. Not. Roy. Astron. Soc. **371**, 867 (2006), arXiv:astro-ph/0604040.

[64] S. P. Oh, Astrophys. J. **553**, 499 (2001), arXiv:astro-ph/0005262.

[65] S. Seager, D. D. Sasselov, and D. Scott, Astrophys. J. Lett. **523**, L1 (1999), arXiv:astro-ph/9909275.

[66] A. V. Belikov and D. Hooper, Phys. Rev. D **80**, 035007 (2009), 0904.1210.

[67] J. R. Pritchard and A. Loeb, Phys. Rev. D **78**, 103511 (2008), 0802.2102.

[68] M. Kuhlen, P. Madau, and R. Montgomery, Astrophys. J. Lett. **637**, L1 (2006), arXiv:astro-ph/0510814.

[69] L. Chuzhoy and P. R. Shapiro, Astrophys. J. **651**, 1 (2006), arXiv:astro-ph/0512206.

[70] B. Ciardi and R. Salvaterra, Mon. Not. Roy. Astron. Soc. **381**, 1137 (2007), 0707.3520.

[71] R. Barkana and A. Loeb, Astrophys. J. **626**, 1 (2005), arXiv:astro-ph/0410129.

[72] I. T. Iliev, P. R. Shapiro, A. Ferrara, and H. Martel, Astrophys. J. Lett. **572**, L123 (2002), arXiv:astro-ph/0202410.

[73] B. Yue, B. Ciardi, E. Scannapieco, and X. Chen, Mon. Not. Roy. Astron. Soc. **398**, 2122 (2009), 0906.3105.

[74] S. P. Oh and Z. Haiman, Mon. Not. Roy. Astron. Soc. **346**, 456 (2003), arXiv:astro-ph/0307135.

[75] R. K. Sheth and G. Tormen, Mon. Not. Roy. Astron. Soc. **308**, 119 (1999), arXiv:astro-ph/9901122.

[76] J. R. Pritchard, A. Loeb, and J. S. B. Wyithe, ArXiv e-prints (2009), 0908.3891.

[77] G. L. Bryan and M. L. Norman, Astrophys. J. **495**, 80 (1998), arXiv:astro-ph/9710107.

[78] S. M. Carroll, W. H. Press, and E. L. Turner, Ann. Rev. Astron. Astrophys. **30**, 499 (1992).

[79] W. H. Press and P. Schechter, Astrophys. J. **187**, 425 (1974).

[80] J. M. Bardeen, J. R. Bond, N. Kaiser, and A. S. Szalay, Astrophys. J. **304**, 15 (1986).